

U.S. DEPARTMENT OF THE INTERIOR
U.S. GEOLOGICAL SURVEY

Kinematic Wave Theory
for Debris Flows

by

M. Arattano¹ and W. Z. Savage²

Open-File Report 92-290

This report is preliminary and has not been reviewed for conformity with U.S. Geological Survey editorial standards (or with the North American Stratigraphic Code). Any use of trade, product, or firm names is for descriptive purposes only and does not imply endorsement by the U.S. Government.

¹ Work performed under memo of understanding with the U.S. Geological Survey.
Current address is
CNR IRPI Str. delle Cacce, 73
10135 Torino ITALY

² Golden, Colorado

CONTENTS

	Page
Abstract	1
Introduction	1
The mathematical model	3
Kinematic wave model for debris flows.	6
Analogies with Weir's (1982) mathematical model.	13
Comparison with debris flow data	14
Discussion	24
Conclusions	29
Appendix I	29
Appendix II.	33
References	37

ILLUSTRATIONS

Figure 1. - Sketch of some possible initial conditions for debris flow initiation and their modeling with kinematic wave theory	7
2. - Characteristics and shock path in x, t plane	10
3. - Location of the monitored channel reach of the Muddy River at Mount St. Helens, Washington (After Pierson, 1986)	17
4. - Longitudinal profile of monitored channel reach of the Muddy River. Gaging stations are indicated by arrows (After Pierson, 1986).	18
5. - Stage hydrographs of multiple surges of Oct. 1, 1981 debris flows. Stations are shown in Fig. 4 (After Pierson, 1986).	19
6. - Stage hydrograph of the first debris flow recorded at station 1A on October 1, 1981 compared with a theoretical hydrograph constructed with kinematic wave theory. The bilogarithmic linear regression of the recorded hydrograph data (Fig. 4) used to calculate the value of k is shown on the top right. The correlation coefficient $r^2 = 0.990$	21
7. - Stage hydrograph of the second debris flow recorded at station 1A on October 1, 1981 compared with a theoretical hydrograph constructed with kinematic wave theory. The bilogarithmic linear regression of the recorded hydrograph data (Fig. 4) used to calculate the value of k is shown on the top right.	

	The correlation coefficient $r^2 = 0.941$. . .	22
8.	- Stage hydrograph of the first debris flow predicted by kinematic wave theory at station 1B (Fig. 4) compared with the recorded hydrograph at the same station (theoretical and recorded hydrographs at station 1A are also shown).	25
9.	- Stage hydrograph of the second debris flow predicted by kinematic wave theory at station 1B (Fig. 4) compared with the recorded hydrograph at the same station (theoretical and recorded hydrographs at station 1A are also shown).	26
10.	- Bilogarithmic linear regressions of hydraulic radius against flow height for four different rectangular sections and respective a and k_1 values.	35
11.	- Bilogarithmic linear regressions of hydraulic radius against flow height for four different trapezoidal sections and respective a and k_1 values.	36

TABLES

Table 1.	- Peak flow heights of the four surges of October 1, 1981 recorded at stations 1A and 1B (Fig. 4). Base flow represents water level in channel previous to passage of debris flow	20
2.	- Final values of H , x_s , t and k and other data for the first and second debris flows of October 1, 1981 calculated from the kinematic wave model	23

KINEMATIC WAVE THEORY FOR DEBRIS FLOWS

by

M. Arattano and W.Z. Savage

ABSTRACT

We present a mathematical model for debris flows, based on kinematic wave theory, and apply our model to published data from two debris flows that occurred in 1981 on Mount St. Helens. The model, which is based on a relationship originally developed for water flow in open channels, shows good agreement with the field data.

INTRODUCTION

Debris flows are mixtures of water and highly concentrated dispersions of very poorly sorted sediment (up to boulder-sized particles) that often move at very high speeds and have great destructive power (Pierson, 1986, Takahashi, 1978). Debris flows usually appear as waves (surges) with a steep front. The steep front consists largely of boulders, which can be surprisingly large and which move as though they were on top of the tread of a tractor (Johnson, 1970). Behind the bouldery front the number of boulders gradually decreases and the surge becomes charged with pebble-sized fragments and then more and more diluted until it appears as muddy water (Johnson, 1970; Costa and Williams, 1984).

Debris flows have been modeled as dilatant fluids using Bagnold's (1954) dilatant fluid concept (Takahashi, 1978 and 1980), and as Bingham (1922) plastic fluids (Yano and Daido, 1965; Johnson, 1970; Rodine and Johnson, 1976). Chen (1987 and 1988) has recently reviewed Japanese concepts for modeling debris flows and has formulated a generalized viscoplastic fluid model for these flows.

Debris flows have also been described successfully by models originally developed to simulate surface water flows (Laenen and Hansen, 1988). The water flow models, other than generating useful information about the possible evolution of debris flows, allow at the very least comparison between water flow behavior and the flow behavior of debris.

At this time little is known about the details of initiation of debris flows. For example, debris flows can be triggered by

volcanic eruptions, by landslides, and by failure of natural dams (Pierson, 1986). In some cases it has been possible to reconstruct the conditions for debris flow initiation and to find a close analogy with dam-break phenomena (Gallino and Pierson, 1984). This, of course, is particularly true if a debris flow initiates during failure of a natural dam.

Dam-break phenomena have been analyzed using kinematic wave theory (Hunt, 1982). Kinematic waves are a distinctive type of wave motion that arises in one-dimensional flow problems. Kinematic wave properties follow directly from the continuity equation causing these waves to be distinct from classical wave motions. Classical wave motions depend on the complete momentum equation and are, therefore, called dynamic and possess at least two wave velocities at each point. Kinematic waves possess only one wave velocity. Therefore dynamic waves can move in two directions from their source while kinematic waves move only in one direction (Lighthill and Whitham, 1955).

Kinematic wave theory is presented in detail by Lighthill and Whitham (1955). They show that, for Froude numbers, $F_r < 2$, kinematic waves follow dynamic waves at a lower speed. However, since dynamic waves rapidly decay, kinematic waves assume the dominant role in disturbance propagation far from the source. Also, kinematic waves develop steep shock fronts that are a consequence of overtaking of slower waves by faster waves (Lighthill and Whitham, 1955).

Lighthill and Whitham (1955) discuss, in particular, the asymptotic behavior of a finite volume of water interacting with an infinite volume of water and show that nonlinear interactions and shock confluence result in the loss of information concerning initial conditions. Weir (1982 and 1983) models the asymptotic behavior of kinematic waves of finite volume in dry channels and applies his model to lahars. Weir (1983) emphasizes that since information concerning initial conditions is lost in kinematic wave theory, this theory can be particularly useful in describing natural phenomena in which initial conditions may not be known.

In this paper we will show that, regardless of the cause of initiation, the subsequent behavior of debris flows can be described by a model similar to a model developed for the movement of floodwaves resulting from a dam-break. The dam-break model by Hunt (1982), based on kinematic wave theory, applies at large distances downstream from a failed dam. We modify this model, originally developed for flow in wide rectangular channels, to account for flow in the narrow channels in which debris flows generally occur.

We also show the analogies between our model and Weir's

(1982) model for lahars. Weir (1982) uses kinematic wave theory, with discharge instead of flow height as the dependent variable in the continuity equation. Thus, Weir's model cannot be used when only flow height is available and discharge is unknown. Weir's (1982) model was used by Pierson (Pierson and others, 1990) to reconstruct the propagation of the catastrophic lahars triggered by the Nevado del Ruiz eruption of 13 November 1985.

We have applied our model to data collected on October 1, 1981 from two gaging stations along a reach of a stream channel on Mount St. Helens (Pierson, 1986). The model shows very good agreement with some of the observed data.

THE MATHEMATICAL MODEL

One-dimensional, unsteady flow in a rectangular channel with a fixed slope is described by the momentum equation,

$$uu_x + u_t + gh_x = gi - gi_f \quad (1)$$

and the continuity equation (Abbott, 1966),

$$h_t + uh_x + hu_x = 0 \quad (2).$$

In these equations (known as De Saint Venant equations) t is time; g is the gravitational acceleration constant; u is velocity; x is distance along the channel; i is channel slope; h is flow height; and i_f is the bed resistance term. The x and t subscripts denote partial derivatives.

Equations (1) and (2) are derived for an infinitesimal element of fluid of unit width. The first two terms in equation (1) represent the Eulerian acceleration over the element while the third term represents the potential gradient over the element. The first term in equation (2) represents the accumulation within an element and the last two terms the net inflow into the element.

Dimensionless variables are introduced in the following in order to put equation (1) into a form involving quantities that can be neglected. The dimensionless variables we introduce are:

$$h_* = \frac{h}{H} \quad x_* = \frac{x}{L} \quad (3),$$

$$u_* = \frac{u}{U} \quad t_* = \frac{Ut}{L} \quad (4),$$

where L is a typical length, H is a typical flow height, and U is a typical velocity in the flow. Using dimensionless variables the momentum and continuity equations become

$$\frac{U^2}{gL} \left[u_* \frac{\partial u_*}{\partial x_*} + \frac{\partial u_*}{\partial t_*} \right] + \frac{H}{L} \frac{\partial h_*}{\partial x_*} = i - i_f \quad (5),$$

and

$$\frac{\partial h_*}{\partial t_*} + h_* \frac{\partial u_*}{\partial x_*} + u_* \frac{\partial h_*}{\partial x_*} = 0 \quad (6).$$

For our problem (see equation 12) the term $\frac{U^2}{gL}$ can also be

written as $\frac{iU^2}{gH}$. The term U^2/gH , which is the square of the

Froude number, F , is a measure of the relative importance of kinetic and potential energy in the flow.

In kinematic wave theory it is assumed that the product of the Froude number and the acceleration terms and the product of the ratio H/L and the flow height gradient term in equation (5) are negligible. Equation (5) then becomes simply:

$$i_f = i \quad (7)$$

and the flow is described by equation (6). Hunt (1982), in his kinematic wave analysis of the dam-break problem, shows that,

when $F_f < 2$, which is almost always true far downstream, the

neglected terms in equation (5) are less than 10 percent of the channel slope term after the floodwave front has traveled a distance of 5.2 times the length of the original dammed reservoir.

In hydraulics we have an empirical relationship between discharge, Q , and flow height, h ,

$$Q = vh^\eta .$$

where v and η are constants.

We also know that discharge is the product of velocity and flow cross-sectional area. Since the data we will use are in terms of flow height, we assume an analogous relationship between velocity and flow height. In fact, we show in appendix I that the velocity u can be written as a function of flow height h (equation A9). Equation (A9) in dimensionless terms becomes

$$u_* = h_*^k \quad (8),$$

As we show in appendix II, the value of k depends on the width of the flow cross-section. Since $R = h$ for an infinitely wide rectangular section we have from equation (A5) and (A7b) that k is $2/3$. For a rectangular flow cross-section of zero width, k is zero. Thus for rectangular channels that have a width between 0 and ∞ k ranges between 0 and $2/3$.

Differentiating equation (8) partially with respect to x_* we obtain

$$\frac{\partial u_*}{\partial x_*} = kh_*^{k-1} \frac{\partial h_*}{\partial x_*}$$

and the second term in equation (6) becomes

$$h_* \frac{\partial u_*}{\partial x_*} = kh_*^k \frac{\partial h_*}{\partial x_*} = ku_* \frac{\partial h_*}{\partial x_*} \quad (9).$$

Substituting this expression in equation (6) gives the continuity equation as

$$\frac{\partial h_*}{\partial t_*} + (k+1)u_* \frac{\partial h_*}{\partial x_*} = 0 \quad (10).$$

Equation (10), which governs the propagation of perturbations in flow height, in dimensional form is

$$h_t + (k+1)uh_x = 0 \quad (11).$$

In appendix I, by using the reduced form of the momentum equation (equation 7) and the Manning equation (equation A1), we have defined a simple relationship between velocity and flow height given as equations (A9) or (8). Then using this relationship in the continuity equation we have just derived a single first order equation governing the propagation of perturbations in flow height (equation 11). In the next section we will use equation (11) as the governing equation for modeling debris flows as kinematic waves.

KINEMATIC WAVE MODEL FOR DEBRIS FLOWS

A possible condition for debris flow initiation is sketched in Fig. 1. The debris mass from which the debris flow develops is represented to be like a water mass behind a dam before collapse. Again we emphasize that initial conditions like those sketched in Fig. 1 are not particularly important to the later behavior of debris flows when these flows are modeled as kinematic waves. Hence the choice of initial conditions is somewhat arbitrary. We also show in Fig. 1 the meaning of the parameters H and L that are used in what follows. The maximum initial (undisturbed) height of debris in the channel is H. The parameter H is analogous to the water height immediately behind an unbreached dam. The initial undisturbed length of the debris mass in the channel is L. The parameter L is analogous to the reservoir length behind an unbreached dam. Since a constant channel slope is assumed, the H and L parameters are linked by the relation

$$i = \frac{H}{L} \quad (12).$$

Referring to Fig. 1, we see that the flow height $h(x,t)$ in equation (11) is subject to the initial conditions,

$$h(x,0) = \frac{H}{L}x \quad \text{for } 0 \leq x \leq L$$

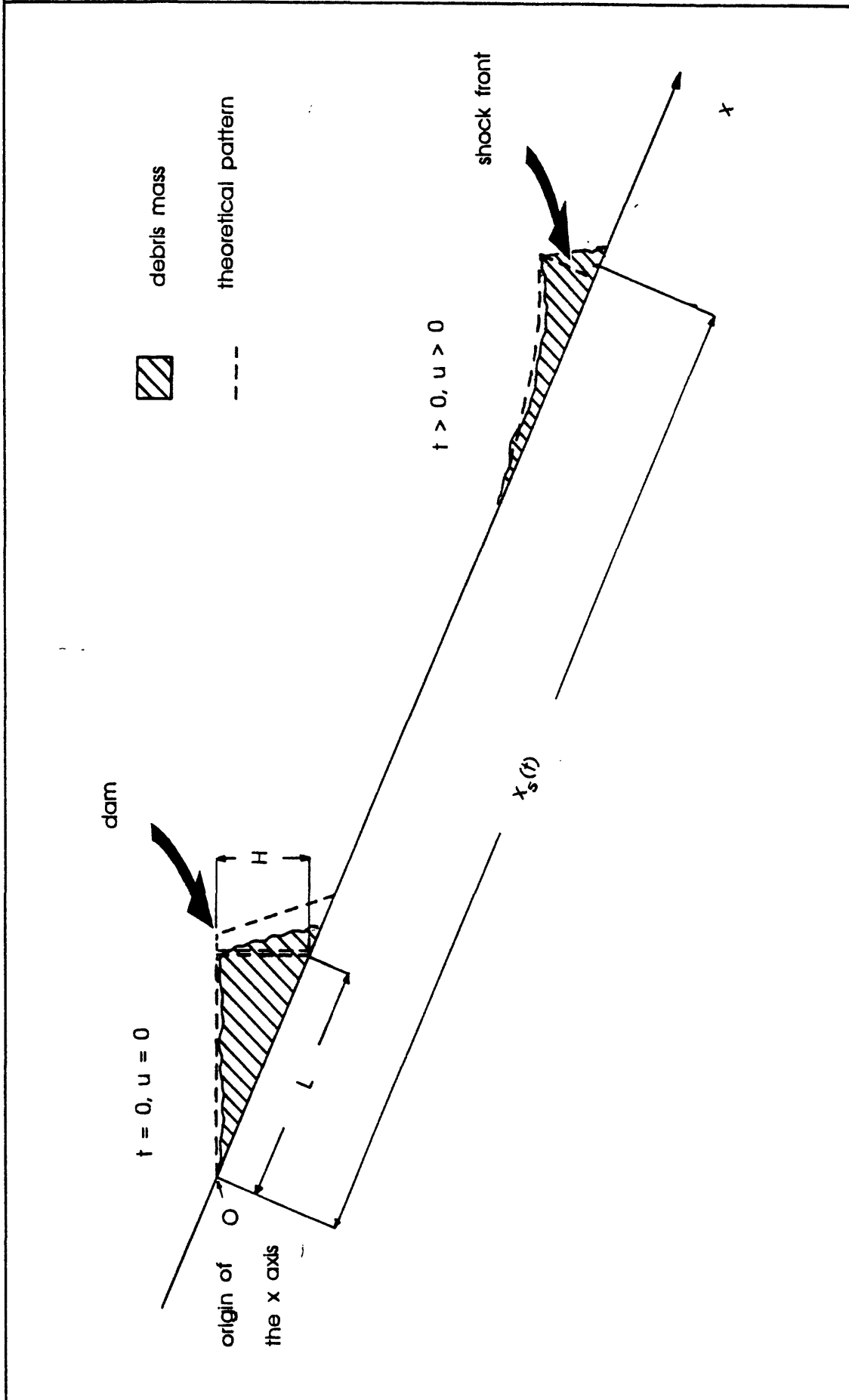


Figure 1. - Sketch of some possible initial conditions for debris flow initiation and their modeling with kinematic wave theory.

$$h(x,0) = 0 \quad \text{for } -\infty < x < 0 \quad \text{and} \quad L < x < +\infty \quad (13).$$

Kinematic theory predicts that a shock front will develop at the front of the debris flow during its motion. We require, $x_s(t)$, the location of the shock front, to move with the speed of the fluid immediately behind the shock, that is,

$$\frac{dx_s(t)}{dt} = u(x_s(t),t) \quad (14),$$

where

$$x_s(0) = L \quad (15).$$

Equation (15) is the initial condition for differential equation (14).

Omitting the asterisk subscript for notational convenience, equations (8) and (10) and conditions (13), (14), and (15) can be rewritten as,

$$u = h^k \quad (16),$$

$$h_t + (k+1)h^k h_x = 0 \quad (17),$$

where

$$h(x,0) = x \quad \text{for } 0 \leq x \leq 1$$

$$h(x,0) = 0 \quad \text{for } -\infty < x < 0 \quad \text{and} \quad 1 < x < +\infty \quad (18),$$

and

$$\frac{dx_s(t)}{dt} = h^k(x_s(t),t) \quad (19),$$

where

$$x_s(0) = 1 \quad (20).$$

Solving equation (17) by the method of characteristics (Abbott, 1966) we find that

$$\frac{dh}{dt} = 0 \quad (21)$$

along characteristic curves that have the slope given by

$$\frac{dx}{dt} = (k+1)h^k \quad (22).$$

Equations (21) and (22) are both ordinary differential equations that are integrated to give

$$h = C_1 \quad (23)$$

along the characteristic curves given by

$$x - (k+1)h^k t = C_2 \quad (24).$$

Here C_1 and C_2 are constants of integration and k is constant along the channel. Note from the Appendices that k is constant because no abrupt change in cross-sectional form is assumed for the flow.

Using the initial condition (18), we can calculate the integration constant for any characteristic curve. In the (x,t) plane (Fig. 2) a characteristic curve given by equation (24) intersects the x axis at $x = x_0$ (where $0 < x_0 < 1$) when $t = 0$. Thus for $t = 0$ equation 24 gives the integration constant

$$x = x_0 = C_2$$

and equation (24) becomes

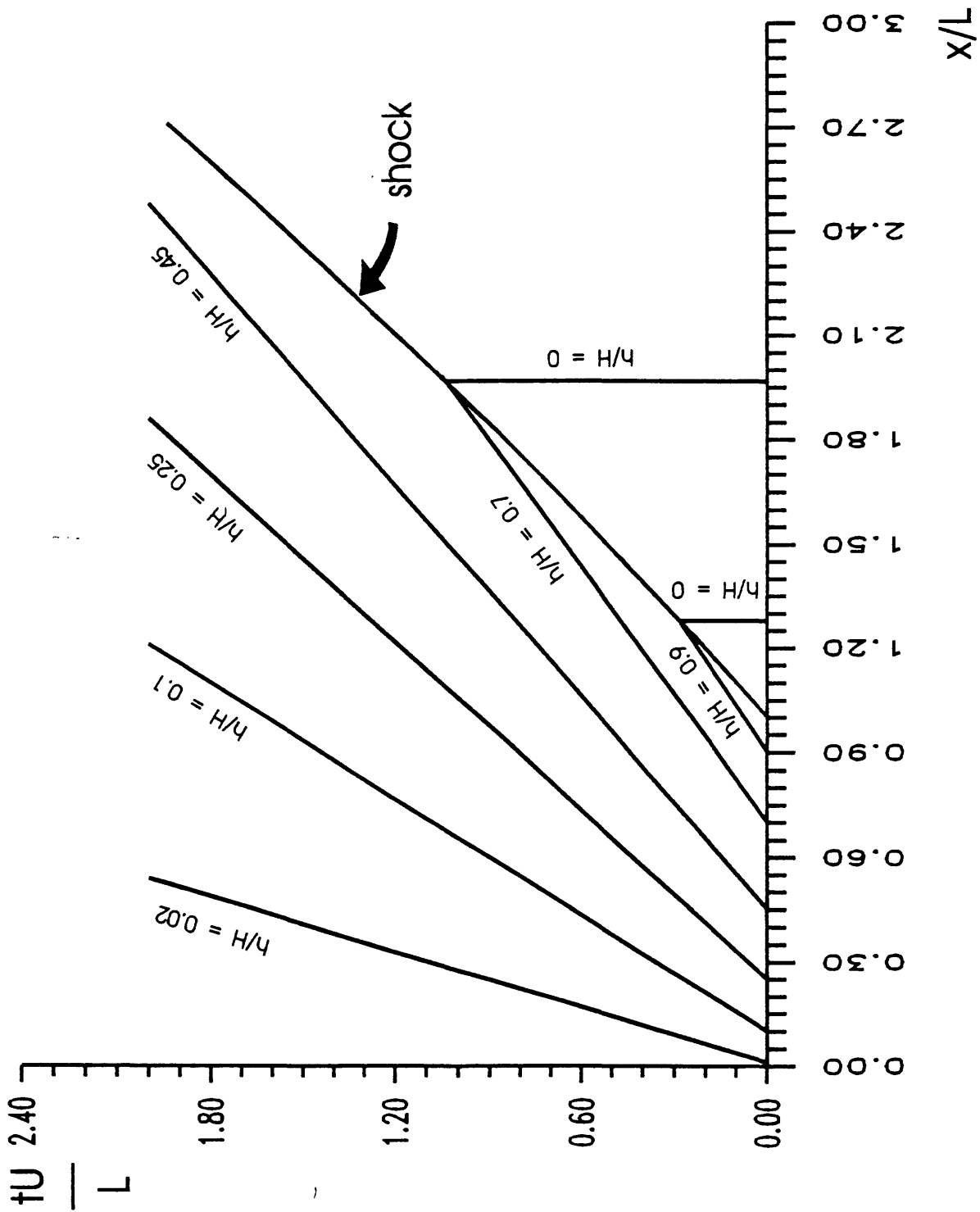


Figure 2. - Characteristics and shock path in x, t plane.

$$x - (k+1)h^k t = x_0 \quad (25).$$

Recall from equation (18), that the dimensionless flow height $h(x,0)$, obtains the value

$$h(x,0) = x \quad \text{for } 0 \leq x \leq 1 ;$$

that is,

$$h = x_0 \quad (26).$$

Eliminating the parameter " x_0 " from equations (25) and (26) we find the characteristic curve equation,

$$x - (k+1)h^k t = h \quad (27).$$

Equation (27) represents a straight line in the (x,t) plane. The characteristic curves are thus straight lines and along each curve the flow height, h , has a constant value. They leave the x axis along the interval $0 < x < 1$, as an expansion fan in the (x,t) plane (Fig. 2). Outside this interval, along the x axis, the flow height is zero, as we can see from initial conditions (18), and the characteristic curves leaving the x axis are straight lines parallel to the t axis.

The intersection of the two families of characteristic curves gives the position of the shock, which must be inserted in the solution to prevent the physically absurd situation of two different flow height values at the same point. The position of the shock can be found analytically by assuming that debris volume is conserved during the process (Weir, 1982, 1983; Hunt, 1982).

Defining A to be debris volume per unit cross-sectional width we then have,

$$\int_0^{x_s(t)} h(x,t) dx = A \quad (28),$$

for debris-volume conservation. Remembering the meaning of the H and L parameters (Fig. 1), we can write

$$A = \frac{1}{2}HL \quad (29).$$

Using equation (29) in equation (28) and writing equation (28) in dimensionless variables we get

$$\int_0^{x_s(t)} h(x,t) dx = \frac{1}{2} \quad (30).$$

As shown by Hunt (1982), equation (30) is easily integrated when equation (27) is used to change the integration variable from x to h ; that is,

$$dx = (1+k(k+1)h^{k-1}t)dh \quad (31).$$

Thus equation (30) takes the simple form,

$$\int_0^{h_s(t)} (h+k(k+1)h^k t) dh = \frac{1}{2} \quad (32),$$

in which $h_s(t)$ is the flow height immediately behind the shock.

Treating the variable t as a parameter, assuming k as constant, and calculating the integral of (32), we can solve the result for t giving,

$$t_s = \frac{1-h_s^2}{2kh_s^{k+1}} \quad (33).$$

The x coordinate of the shock can then be found by eliminating the variable t from equations (27) and (33) to give

$$x_s = \frac{k+1}{2kh_s} - \frac{1-k}{2k} h_s \quad (34).$$

Equations (33) and (34) are thus parametric equations of the shock front in the (x,t) plane. The solution in the region between the shock front and the t -axis is given by equation (27), while outside of this region the solution is given by $h = 0$ (Fig.

2). Far from the origin, for large times and behind the forward shock, the characteristic curves that define the wave appear to originate approximately from the origin, which shows graphically the relative lack of importance of initial conditions to subsequent, late-time, kinematic wave propagation.

ANALOGIES WITH WEIR'S (1982) MATHEMATICAL MODEL

Equation (27) can be rewritten as

$$1 - \frac{h}{x} = \frac{(k+1)h^k t}{x} \quad (35)$$

for large x fluid height, h , is small, and thus $\frac{h}{x}$ is small so equation (27) can be approximated by

$$h = \left(\frac{x}{k+1}\right)^{\frac{1}{k}} t^{-\frac{1}{k}} \quad (36)$$

Equation (36) shows that at a fixed point, x , water depth, h , varies as $t^{-\frac{1}{k}}$.

Weir (1982), using kinematic wave theory and an asymptotic solution valid for large times, has also shown discharge of lahars to vary as a negative power of time. Weir (1982) arrives at the expression

$$q = \left[\frac{f(x)}{t}\right]^{\frac{\kappa}{\kappa-1}} \quad (37)$$

where κ is a constant parameter and $f(x)$ is a complicated function

of x . Thus at a fixed point, x , discharge varies as $t^{-\frac{\kappa}{\kappa-1}}$. Weir (1982) accounts for changing slope in his model by defining slope as px^{-r} .

COMPARISON WITH DEBRIS-FLOW DATA

When modeling lahars, eruption time can be determined from seismic records and the value of the variable t to be used in equation (36) is then also known. In fact, Weir (1982) uses such information in his equation describing the change of discharge with time for lahars.

For debris flows we normally do not know the time of flow initiation. However this difficulty can be resolved by installing two gaging stations at a fixed distance along the channel.

Knowing the distance " l " between the two stations and adopting the same value of k for both cross sections, we can then write equation (34) in dimensional form for the two stations as the two equations (the subscript for x has been omitted)

$$\frac{x}{L} = \frac{k+1}{2k} \frac{(1-k)h_1}{H} \quad (38)$$

and

$$\frac{x+l}{L} = \frac{k+1}{2k} \frac{(1-k)h_2}{H} \quad (39)$$

in which h_1 and h_2 are the peak flows at the first and second

stations, respectively, l is the distance between the two gaging stations, and x is the unknown distance of the first gaging station from the origin of the flow. We can express the parameter

L in equations (38) and (39) as a function of channel slope, i , and initial height, H , by equation (11). Equations (38) and (39) then give a system of equations for the unknowns H and x . Solving this system we get the following expressions for H and x as functions of k :

$$H = \sqrt{\frac{li + \frac{k-1}{2k}(h_1 - h_2)}{\frac{k+1}{2k}(\frac{1}{h_2} - \frac{1}{h_1})}} \quad (40)$$

and

$$x = \frac{1}{i} \left(\frac{k+1}{2kh_1} H^2 - \frac{1-k}{2k} h_1 \right) \quad (41).$$

If we do not know the cross sectional shape and hence k , we can choose a trial value for k (for example 2/3, valid for wide rectangular channels) to get approximate values for H and x from equations (40) and (41). Equation (33) can then be used to

obtain t in dimensionless form; that is $t_s = \frac{1-h_s^2}{2kh_s^{k+1}}$, where h_s , the shock height, is equal to the peak flow height.

To express t in dimensional form we use the definition of nondimensional time (equation 4). This requires that we know U

and L , where U is given by $U = CH^k i^{\frac{1}{2}}$ (equation A10) and L is given

by $i = \frac{H}{L}$ (equation 12). To calculate C , we use mean values of peak velocities and flow heights at stations 1 and 2 in equation

(A7), $u = Ch^k i^{\frac{1}{2}}$. Then solving for C , and assuming C to be constant with flow height, we have U and hence dimensional t , which represents a value for the elapsed time since debris flow initiation. This value of t gives an estimated time, t_e , for the appearance of the debris flow at the first gaging station.

If equation (36) is plotted with $\log h(t)$ as the ordinate and $\log t$ as the abscissa, then, for fixed x , a straight line

with slope $-\frac{1}{k}$ results. If we find that a plot of the logarithm

of the hydrograph data collected at the first gaging station, that is $\log h(t)$, against the logarithm of time, $\log t$, (starting

from the time t_c) can be approximated as a straight line with negative slope, then we can estimate a value for k. The use of this value for k in equations (40) and (41) then gives improved values for H and x and we can repeat the calculations. The iteration is rapidly convergent and gives final consistent values for H, x, t and k. Finally, having determined the parameters necessary to predict the hydrograph beyond the first gaging station, we can predict the hydrograph at the second gaging station and compare it with the recorded hydrograph at that station.

To test our model we have used data (Pierson, 1986) recorded in 1981 in a reach of the Muddy River immediately downstream from the terminus of the Shoestring Glacier, on the southeast flank of Mount St. Helens (Fig. 3). Among the many different methods used for debris-flow monitoring at this site, there are two gaging stations separated by a distance of 273 m. Between the two stations (labeled with 1A and 1B in Fig. 4) the channel slope is approximately constant (about 0.184 radians) except for the 10-m-high falls shown in Fig. 4.

On 1 October 1981, four debris flows occurring a few minutes apart were recorded at gaging stations 1A and 1B. The first two surges had peak flows at the first station of 3.36 m and 2.36 m (Fig. 5), respectively. Using the original hydrographs and the data shown in Table 1, we have calculated by the procedure outlined above values of H, x, t and k for these first two surges. Values of h_1 and h_2 used in the calculation are given in Table 1. These flow heights are peak flow height values above the channel bottom.

Hydrographs for the first and second debris flows recorded at the first station (1A) are shown in Figs. 6 and 7 together with theoretical hydrographs predicted by kinematic wave theory. The values of k have been calculated by linear regression of the recorded hydrographs in a bilogarithmic plane. These regressions also are shown in Figs. 6 and 7, and the values of k are in Table 2. In that table we also show values obtained for x, H and L. In both cases the x values, which give an estimate of the distance from the source of the debris flows to the first gaging station, are large enough to apply kinematic wave theory.

We have calculated two approximate values of the Froude

number ($F_r = \frac{u}{\sqrt{gh}}$) using the mean front velocity values and the mean peak flow values between the two stations (Table 1). We see that both values are less than 2 ($F_r = 0.67$ for the first debris-

122°15'
46°
15'

122°7'30"

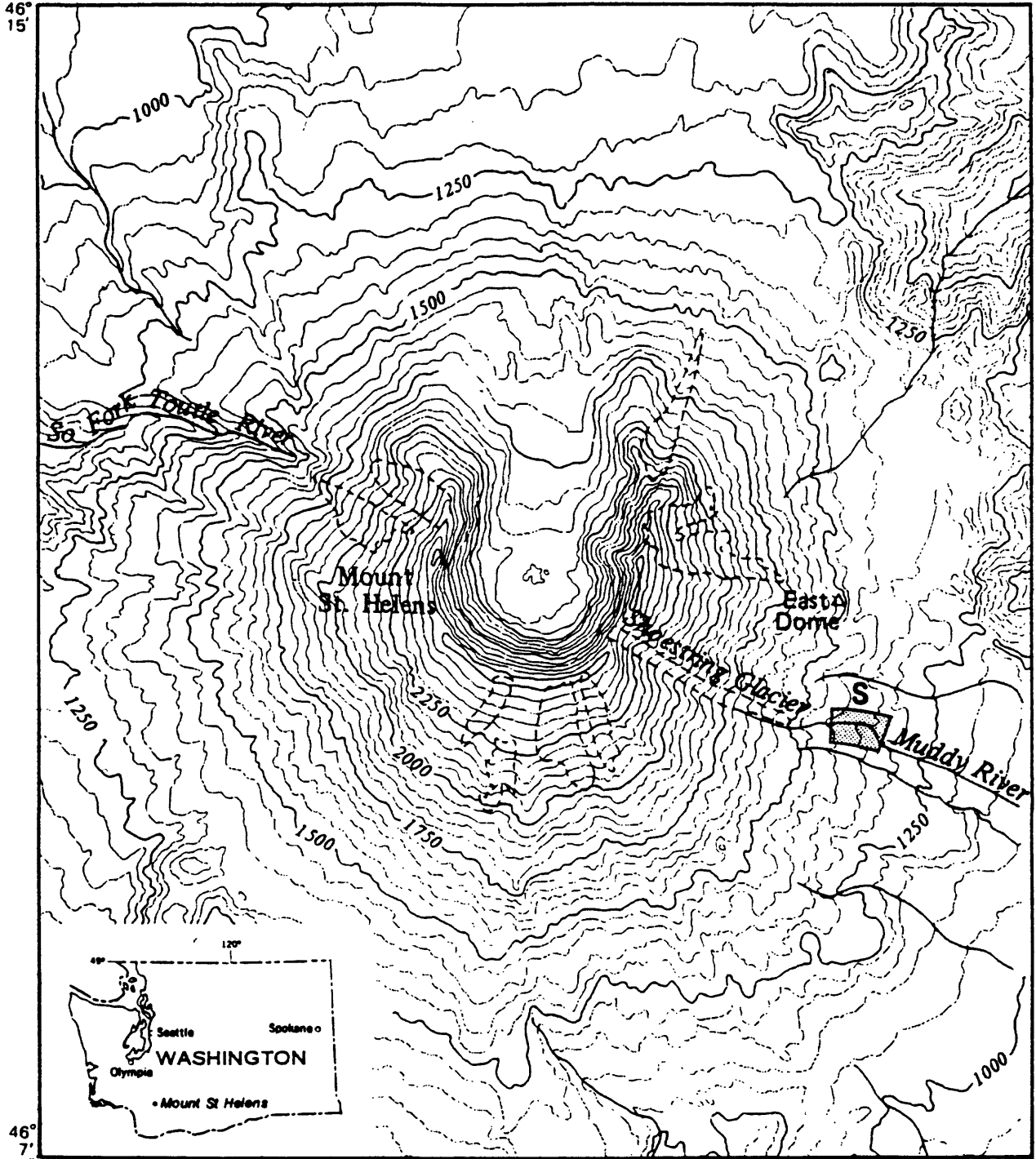


Figure 3. - Location of the monitored channel reach of the Muddy River at Mount St. Helens, Washington (After Pierson, 1986).

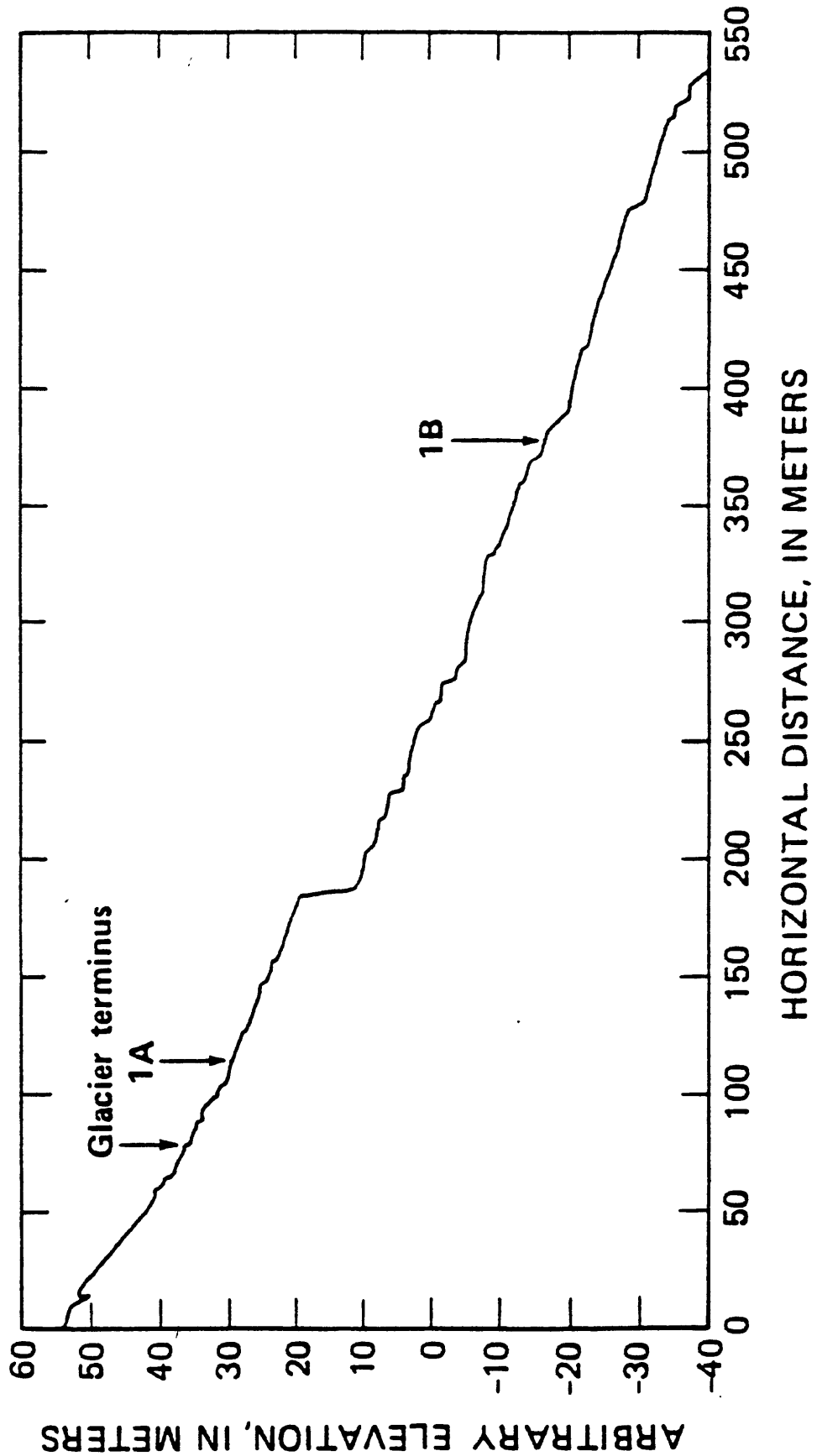


Figure 4. - Longitudinal profile of monitored channel reach of the Muddy River. Gaging stations are indicated by arrows (After Pierson, 1986).

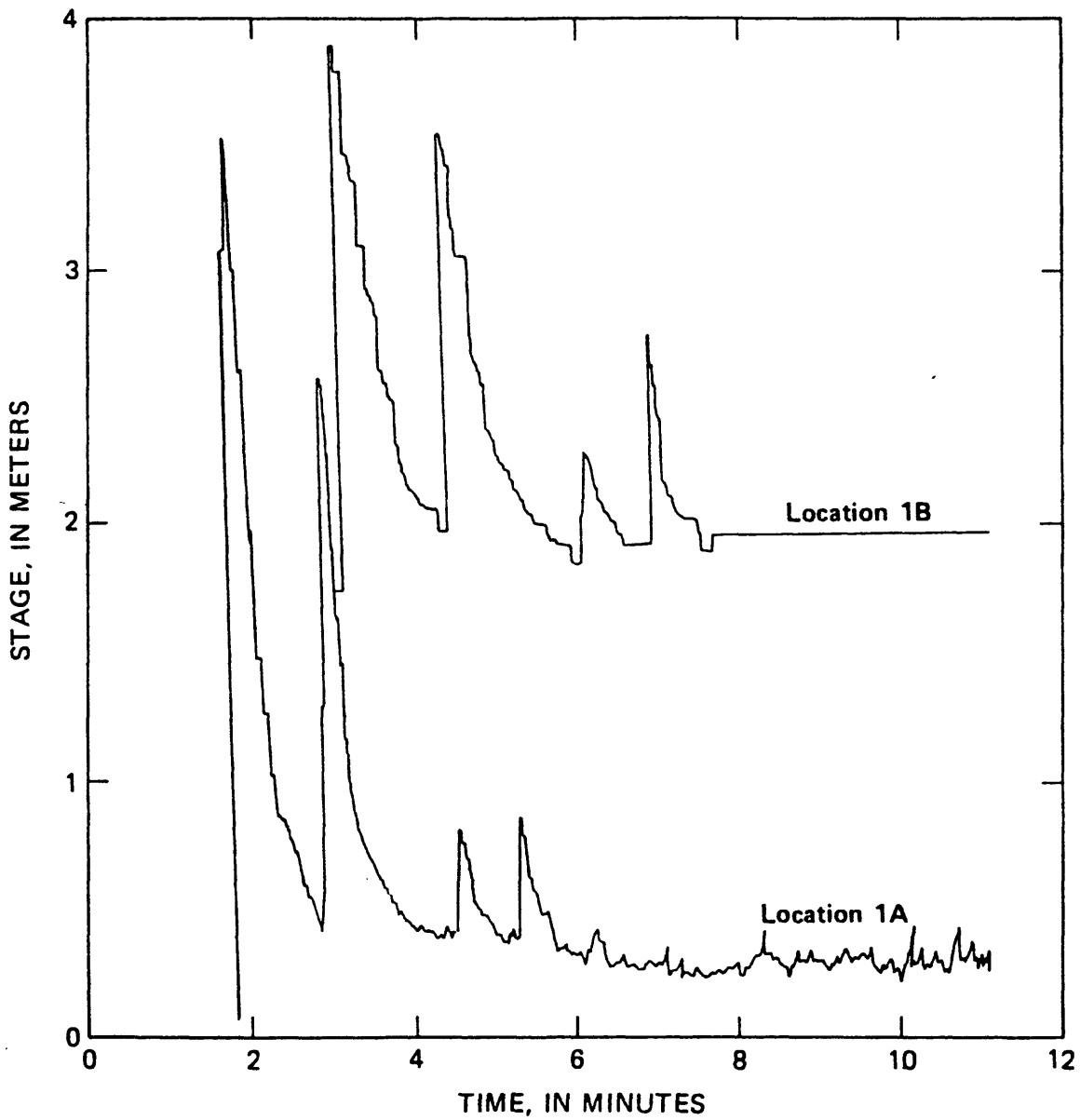


Figure 5. - Stage hydrographs of multiple surges of Oct. 1, 1981 debris flows. Stations are shown in Fig. 4 (After Pierson, 1986).

	1 st debris flow		2 nd debris flow		3 rd debris flow		4 th debris flow	
	a	b	a	b	a	b	a	b
Station 1A	3.36	3.30	2.36	2.20	0.58	0.42	0.62	0.49
Station 1B	2.16	2.13	1.82	1.59	0.51	0.44	1.02	0.85

a peak flow height above channel bottom (m)

b peak flow height above base flow (m)

Table 1 - Peak flow heights of the four surges of October 1, 1981 recorded at stations 1A and 1B (Fig. 4). Base flow represents water level in channel previous to passage of debris flow.

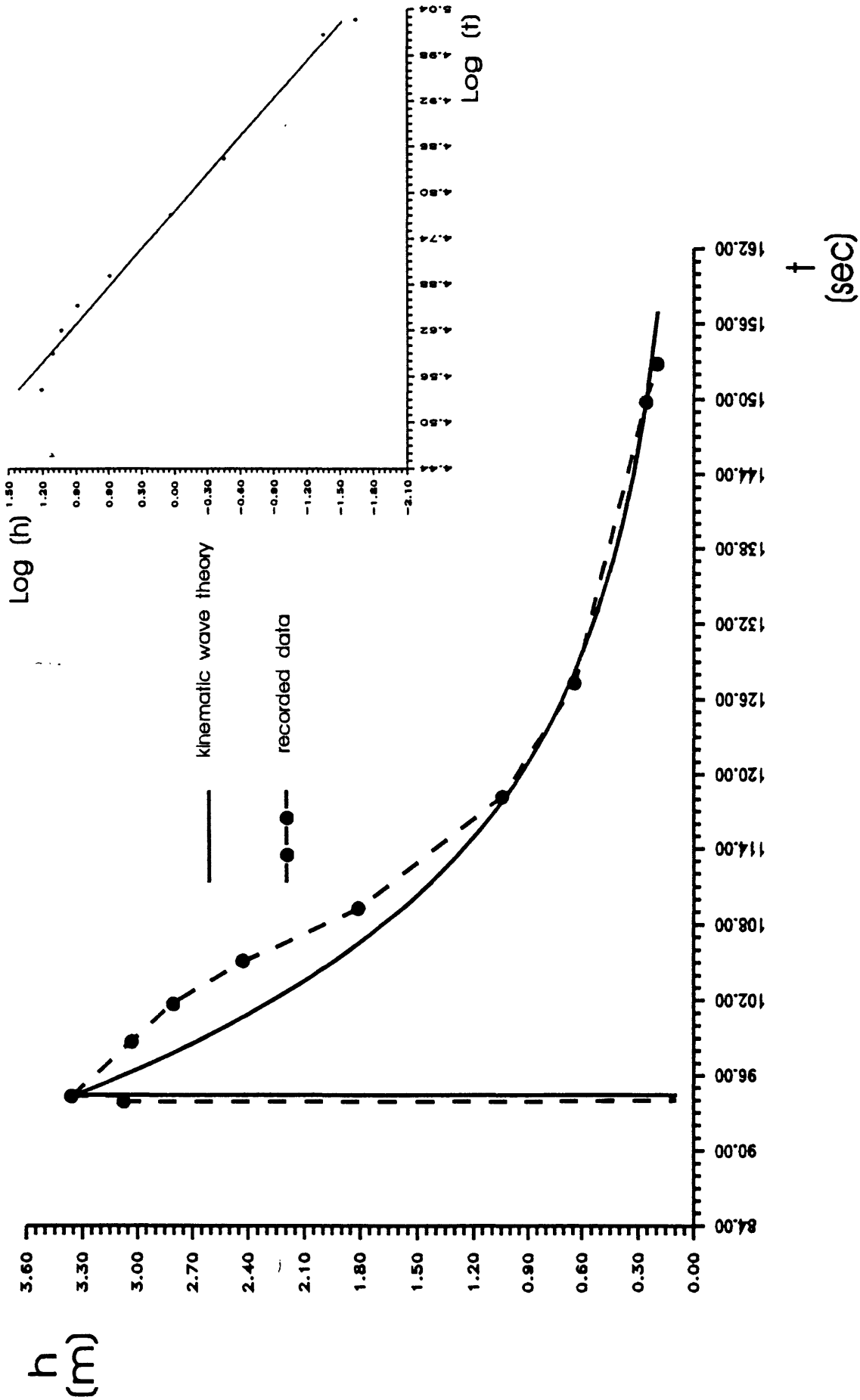


Figure 6. - Stage hydrograph of the first debris flow recorded at station 1A on October 1, 1981 compared with a theoretical hydrograph constructed with kinematic wave theory. The bilogarithmic linear regression of the recorded hydrograph data (Fig. 4) used to calculate the value of k is shown on the top right. The correlation coefficient $r^2 = 0.990$.

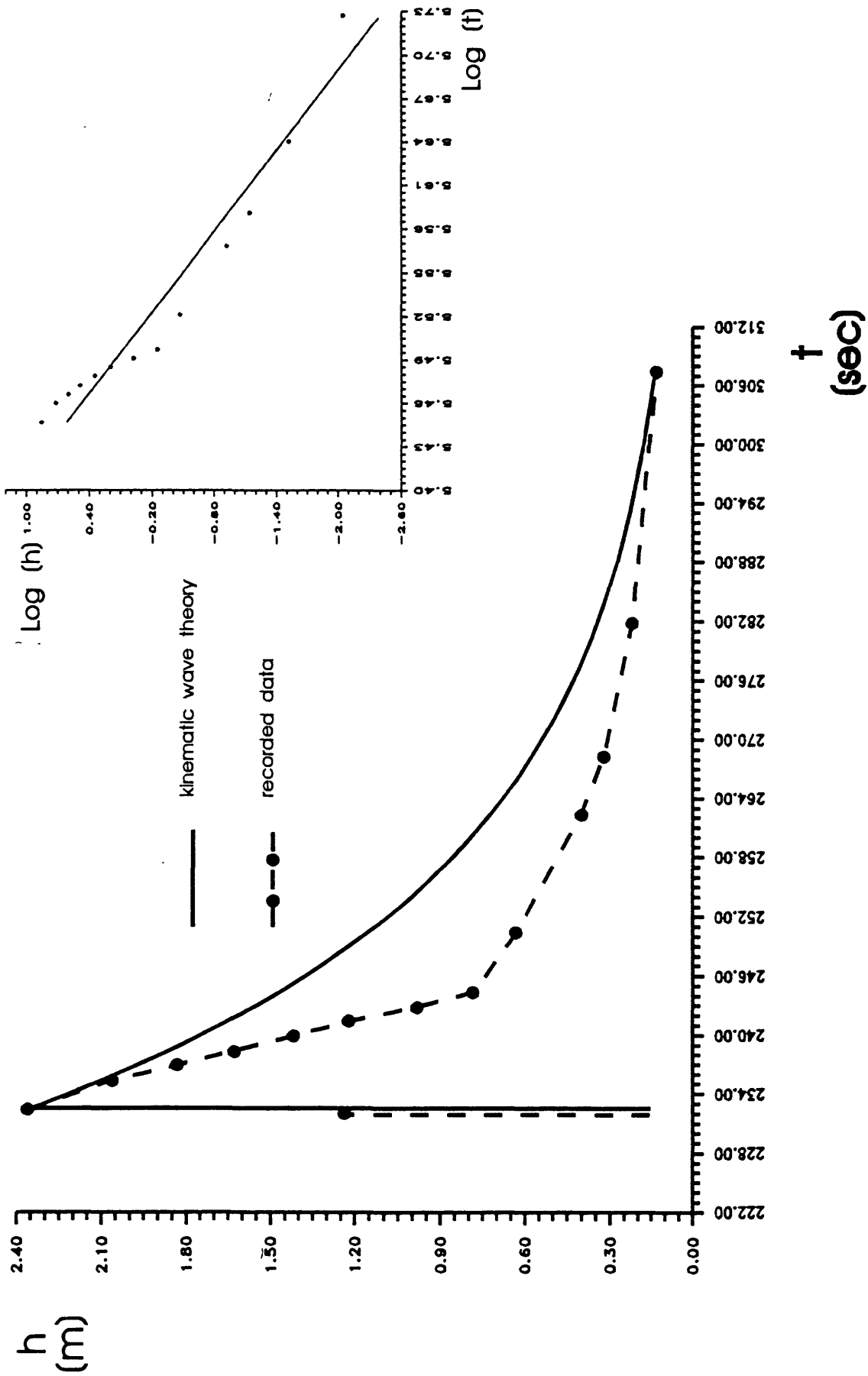


Figure 7. - Stage hydrograph of the second debris flow recorded at station 1A on October 1, 1981 compared with a theoretical hydrograph constructed with kinematic wave theory. The bilinear regression of the recorded hydrograph data (Fig. 4) used to calculate the value of k is shown on the top right. The correlation coefficient $r^2 = 0.941$.

	u [m/s]	Δt [s]	h_1 [m]	h_2 [m]	x [m]	H [m]	L [m]	t [s]	k	C	A [m^2]
1 st debris flow	3.5	78	3.36	2.16	415	8.96	48.7	94	0.16	6.9	217.2
2 nd debris flow	3.1	88	2.36	1.82	809	8.02	43.6	232	0.09	6.7	175.2

u mean velocity between station 1A and 1B

Δt elapsed time between recordings at station 1A and 1B

Table 2 - Final values of H , x , t , k and other data for the first and second debris flows of October 1, 1981.

flow and $F_r = 0.68$ for the second), which is consistent with Hunt's criteria for omitting the derivative terms in equation (5).

Theoretical hydrographs forecast by the model for the first and second debris flows at the first and second gaging stations are shown in Figs. 8 and 9. The theoretical hydrographs show good agreement with recorded data at the gaging stations in both cases.

DISCUSSION

The agreement between measured and theoretical hydrographs in Figs. 8 and 9 implies that debris-flow behavior can be considered to be similar to clear water behavior to which kinematic wave theory and the Manning equation are usually applied. In fact, Pierson (1986) has shown that the Manning equation can be applied to debris flows when sediment concentration is as much as 76-78 percent by weight. Observing debris flows one notices that they become more fluid behind a boulder-laden front and can develop features typical of water behavior such as the hydraulic jump shown by Costa and Williams (1984).

We have no information about channel cross sections at the two stations and hence have been unable to estimate discharge hydrographs for them. Of course, if we knew cross sectional areas we could determine discharge by using equation (A7) to calculate mean velocities for changing flow heights at both sections 1A and 1B.

The assumption of a constant k value along the channel seems to be reasonable for flows 1 and 2. We see that at both stations predicted hydrographs with constant k values show good agreement with the actual debris flows. However, with no information about cross-sectional shape, we have been unable to verify the k values obtained by the procedures outlined above. The k value for the second debris flow is smaller than the k value for the first debris flow. This could occur if the flow cross section was narrowing by deposition, by a reduction in flow height, or a combination of these effects. However, we need to remember that we supposed k to be constant for different flow heights in our theory.

The model allows a prediction of the distance that the debris flow has traveled from its point of inception to the first gaging station, x . Values found for x using equation (41) show that the two debris flows should have started on the Shoestring Glacier at 415 m and 809 m from the first station, respectively. We note that Pierson (1986) has postulated that one source of these flows could be glacier outburst floods.

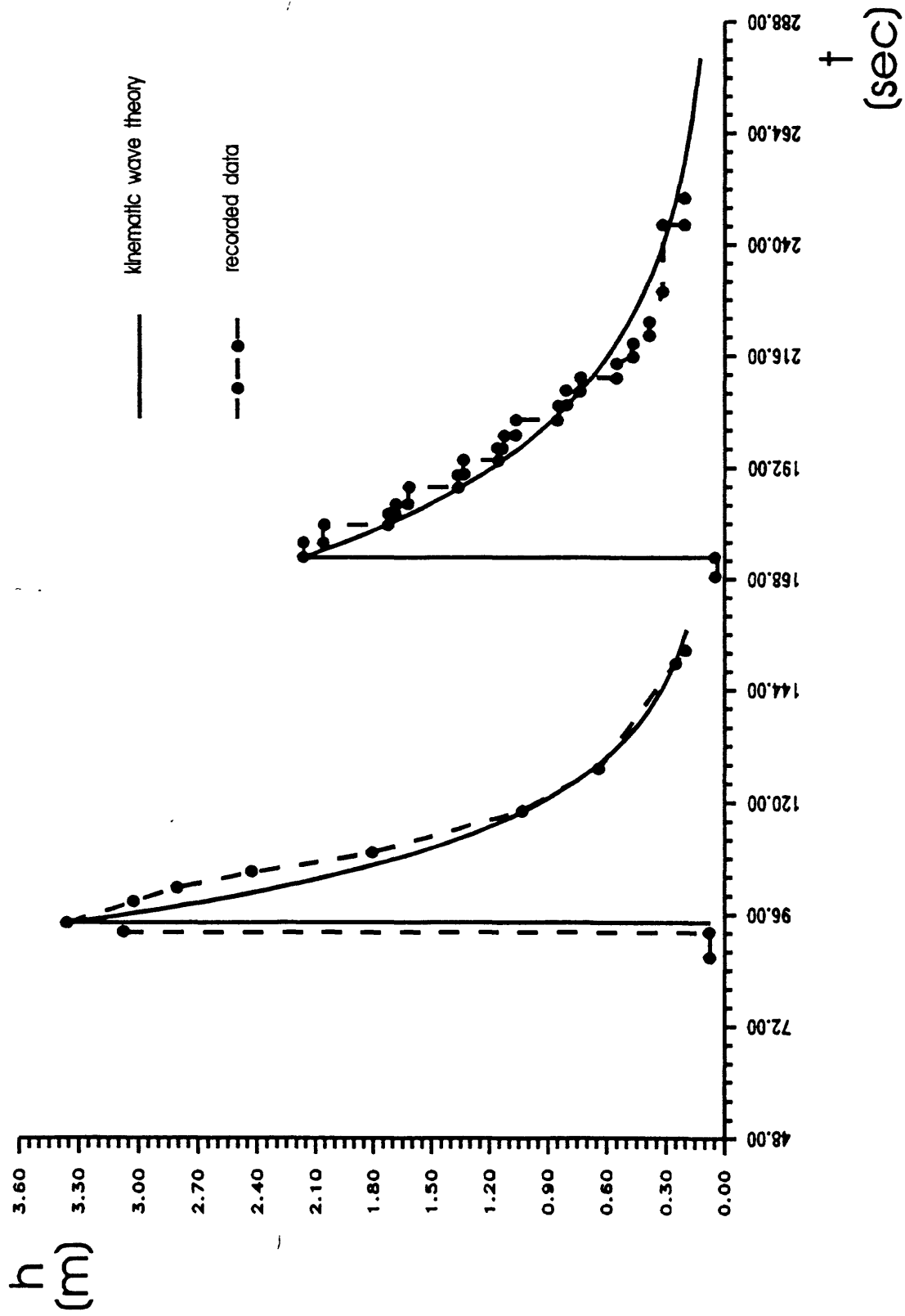


Figure 8. - Stage hydrograph of the first debris flow predicted by kinematic wave theory at station 1B (Fig. 4) compared with the recorded hydrograph at the same station (theoretical and recorded hydrographs at station 1A are also shown).

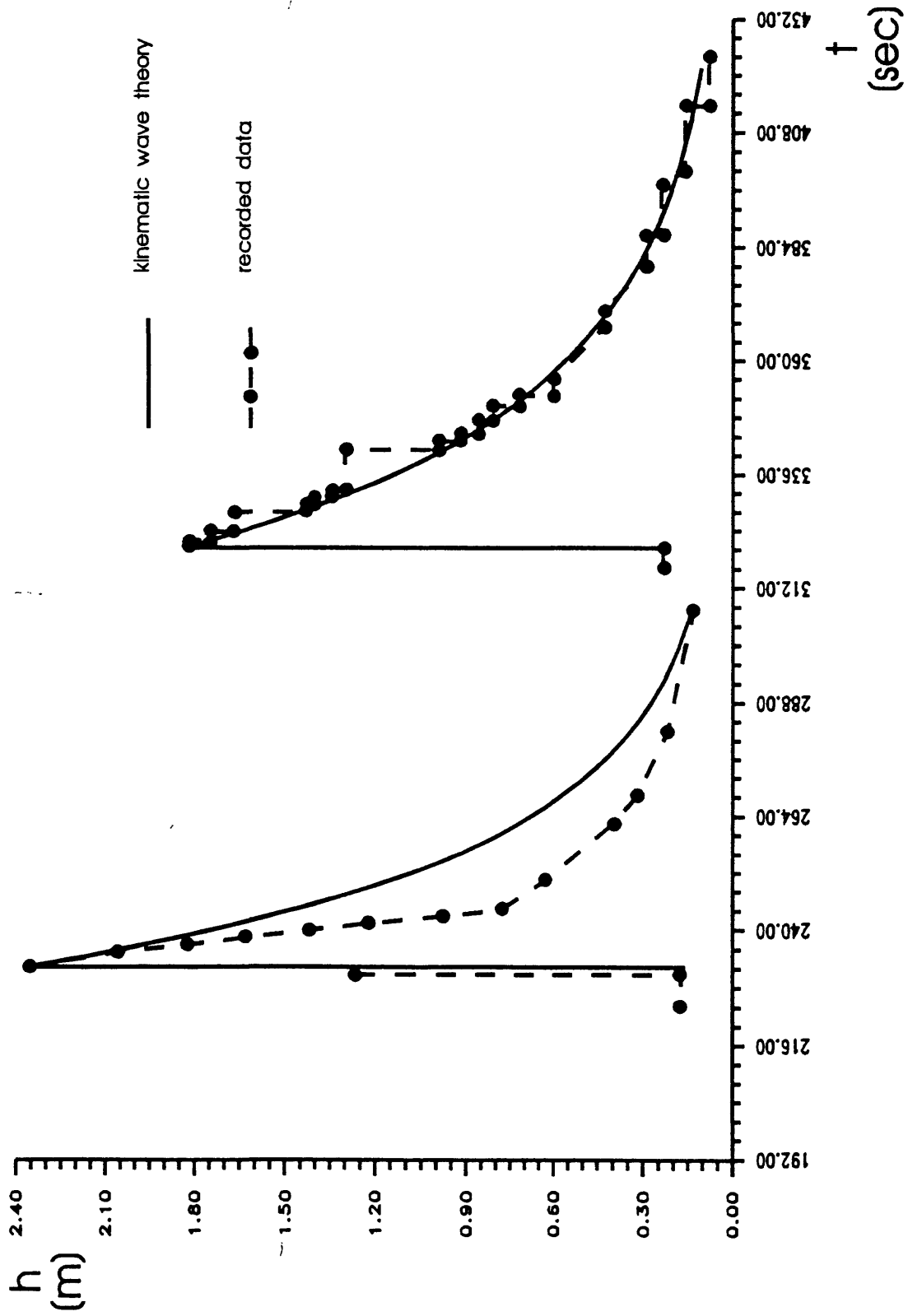


Figure 9. - Stage hydrograph of the second debris flow predicted by kinematic wave theory at station 1B (Fig. 4) compared with the recorded hydrograph at the same station (theoretical and recorded hydrographs at station 1A are also shown).

Also recall that our model does not account for changing slopes. Note in Fig. 4 that the slope in the reach increases upstream, which could affect the estimated values for t , H , x and, thus, k . The model could be improved by taking account of changing slope by using an expression for slope as a function of distance such as that used by Weir (1982).

Note that the linear regression made on recorded hydrograph data at the first station (Fig. 6) would allow an estimation of x , as well as k , from equation (36). However, in both cases, this estimated x value was less than 50 percent of that calculated with equation (41).

More data are needed to show the validity of this model. It would be useful to predict the movement along a stream channel of a known mass of debris caused by a landslide or a previous debris flow. Knowing debris volume, the amount of water required for mobilization, and the mean width of the stream channel, we could calculate the parameter A in equation (28) by dividing the debris and water volume by the mean channel width. Knowing the channel slope, we could then calculate the parameters H and L in equation (29). Also, if we have a value for k and for C along the stream channel we could predict the propagation of the debris flow along the channel.

Our model does not take into account other features of debris flows. For example, debris flows do not show a vertical front but a continuous, rapid rise to peak discharge that may be imperceptible to recorders. Whitham (1955) and Takahashi (1980) derived theoretical expressions to account for the lobate profile of the leading edge of a flow. Actually, Whitham's (1955) equation has been derived to model the profile of the leading edge of a mass of water propagating along a stream channel after a dam failure, while Takahashi's has been derived for debris flows. We have not used such expressions here because of the steep front profile shown by the debris flows examined.

Our model does not allow any prediction about how far debris flows can travel. Theoretically kinematic waves propagate indefinitely. But shock height does decrease downstream until it reaches a practically null value after a finite distance from the starting point.

The model could be improved by using for the term i_f , which accounts for bed resistance, a relationship that accounts for a Bingham behavior (Johnson, 1970) of the debris flow front. This Bingham behavior would account for the apparent strength of the slurry, a strength that would keep the boulders in place at the front of the flow. It would substitute for the relationship we

have adopted for i_f in equation (7), which comes from open-channel-flow theory for water.

The model does not explain the effects of deposition or erosion along the stream channel during flow because it is based on the hypothesis of constant volume. That hypothesis is made when we assume A to be a constant to find the parametric equation of the shock front in the (x,t) plane (equations 33 and 34).

If, because of erosion of deposits along the channel, the peak flow value gets larger during the flow from the first to the second gaging station, the model cannot be applied. This could have happened during the third and fourth debris flows of 1 October 1981 (Fig. 5). Both flows, though much smaller than the first two, show a higher peak flow value at the second station (Table 1). The difference between the peak flow values at the first and second station is particularly large for the fourth surge.

The higher peak flow value at the second gaging station could also be due to an abrupt change in cross-sectional form for small flow heights at that station. If the cross section narrows, we can get a higher peak flow value like the one recorded. But, again, our model cannot account for such a circumstance, since we have supposed the channel cross-sectional form to remain constant along the channel.

A narrow flow cross section, close to a rectangular form, would have a small value for the parameter k and, thus, a narrow hydrograph with a rapid decrease in flow height behind the peak flow value. Thus, rapid decrease of flow height with time would be predicted because small values of k give large exponents in equation (36), causing the flow height, h , to decrease more rapidly with time. An increase of peak flow height at the second station due to a narrower flow cross section that is close to a rectangular form should then show a narrow hydrograph at that station and, indeed, for the last surge, we observe that the hydrograph recorded at the second station is narrower than the one recorded at the first. Kinematic wave theory predicts a continuous spreading out of the hydrograph proceeding downstream, if the value of k does not change along the channel and no mass is added to the flow.

In summary, both erosion and an abrupt change in cross-sectional form of the flow could explain the higher peak flow at the second station and the narrow hydrograph recorded for the last two debris flows. We hope to account for such effects in our future modeling efforts.

CONCLUSIONS

To model debris flows, we have modified a mathematical approach developed from open channel hydraulic theory. This approach was originally used to predict the behavior of a mass of water suddenly released in a wide rectangular stream channel after a dam-break. Our model appears to simulate the form of stage hydrographs from two debris flows that occurred in the Muddy River, on Mount St. Helens, on October 1, 1981, reasonably well. From the hydrographs of these debris flows, recorded by two gaging stations 273 m apart on the stream, we have been able to use the first station hydrograph and the peak flow of the second hydrograph to calculate the model parameters and then forecast the form of the hydrographs at the second station. These forecasts have shown good agreement with actual data, and a behavior of the debris flows examined that is very similar to that of clear water. We have also demonstrated analogies between debris flows and dam-break phenomena. The model has allowed an estimation of the position of the sources of the debris flows and the time of travel of these flows to the first station. Also k values for the channel, k being a parameter that accounts for changes of hydraulic radius with flow depth, have been calculated. If the initial volume of debris is known our model could be used to give a rough forecast of propagation along a stream channel of a debris mass deposited by a landslide or a previous debris flow.

More research is needed to verify the general applicability and reliability of this model. At this time the model cannot include the effects of changing channel slope, nor erosion or deposition during debris flow movement, and it cannot be used to predict the distance that a debris flow can travel. Nevertheless the model provides a quantitative theory that can be useful for future research on debris flows behavior.

APPENDIX I

The Manning equation, originally developed to describe uniform flow of water in open channels, is used in the following to develop an expression for the bed resistance term, i_f , in the momentum equation (equation 1). We show that R , the hydraulic radius, can be expressed in the Manning equation as a function of flow height, h , so that the bed resistance term, i_f , becomes also a function of flow height, h , and, as a consequence, u can also be described in terms of flow height. Expressing the bed resistance term as a function of flow height is essential to the integration of equation (2).

The Manning equation is (Chow, 1959)

$$u = \frac{1}{n} R^{\frac{2}{3}} i^{\frac{1}{2}} \quad (\text{A1}),$$

where

u = mean velocity of the fluid
n = roughness coefficient
R = hydraulic radius
i = channel slope.

Hydraulic radius R is the ratio of cross-sectional area of the flow to the wetted perimeter of the channel (Rouse, 1938). Although hydraulic radius is a function of the cross-sectional flow geometry, the factor R does not fully describe the geometry of the flow cross-section. In fact, R may have the same magnitude for an infinite variety of flow cross-sectional forms (Rouse, 1938).

We now find R as a function of flow height, h. Discharge, Q, for uniform flow in a channel is expressed as the product of the mean velocity of the fluid, u, and water area, S, or, using equation A1, as

$$Q = \frac{1}{n} S R^{\frac{2}{3}} i^{\frac{1}{2}}$$

or

$$Q = K i^{\frac{1}{2}} \quad (\text{A2}),$$

where

$$K = \frac{1}{n} S R^{\frac{2}{3}} \quad (\text{A3}).$$

The term K is known as the conveyance of the channel cross-section, and since K is a function of the depth of flow, h, through S and R, it may be assumed (Chow, 1959) that

$$K^2 = \gamma h^\delta \quad (A4),$$

where γ is a coefficient and δ is called the hydraulic exponent for uniform flow computation (Chow, 1959). For rectangular flow cross-sections of different width, b , Chow (1959) shows

that δ varies within a range of 3.33 to 2 when $\frac{h}{b}$ varies within a range of 0 to ∞ .

However for most channels, except for channels with abrupt changes in cross-sectional form, a logarithmic plot of K as ordinate against the depth h as abscissa will appear approximately as a straight line (Chow, 1959), and

thus δ and γ may be assumed constant for most flow cross-sectional areas.

Since we can express the flow area for any cross-sectional form as a product of a mean width, b , and flow height, h , which is equivalent to approximating the flow cross section with a rectangular flow cross section, we substitute bh for S in equation (A3), and using the resulting expression for K in equation (A4) we obtain

$$R = \frac{n^{\frac{3}{2}} \gamma^{\frac{3}{4}} h^{\frac{3}{4}(\delta-2)}}{b^{\frac{3}{2}}}$$

or as

$$R = ah^{k_1} \quad (A5),$$

which expresses the hydraulic radius R as a function of flow height. Here,

$$a = \frac{n^{\frac{3}{2}} \gamma^{\frac{3}{4}}}{b^{\frac{3}{2}}} \quad \text{and} \quad k_1 = \frac{3}{4}(\delta-2) \quad (A6).$$

For rectangular flow cross-sections, as δ varies from 2 to 3.33, k_1 varies between 0 and 1, depending on the channel width. For most flow cross-sectional areas, except for channels with abrupt changes in cross-sectional form, k_1 , like δ , may be assumed constant.

Substituting equation (A5) in equation (A1) gives:

$$u = Ch^k i^{\frac{1}{2}} \quad (\text{A7a})$$

in which

$$k = \frac{2}{3} k_1 \quad (\text{A7b})$$

and

$$C = \frac{1}{n} a^{\frac{2}{3}} \quad (\text{A7c}).$$

Solving equation (A7) for the channel slope, i , and recalling that because of the kinematic wave approximation, $i = i_f$, we have

$$i_f = \frac{u^2}{C^2 h^{2k}} \quad (\text{A8})$$

for the bed resistance term i_f . Rearranging equation (A7) we have

$$\frac{u}{U} = \left(\frac{h}{H}\right)^k \quad (\text{A9}),$$

that is, the dimensionless relationship between velocity and flow height in which the typical velocity is given by

$$U = CHk_1^{\frac{1}{2}} \quad (\text{A10})$$

and H is a typical height of flow.

We emphasize that the coefficient C in equation (A7) is more than a roughness coefficient. In fact, it is given

by $C = \frac{\gamma^{\frac{1}{2}}}{b}$ where the roughness coefficient, n, is hidden in the

coefficient γ (equation A4). Since the mean flow area width, b, is generally a function of flow height, C becomes a function of flow height. Thus assuming C to be constant can be a rough approximation.

Sometimes debris flows start on unbroken hillsides and cut V-shaped channels (Varnes, 1978), and in many other cases the flow cross-sectional form is close to a triangular form. For a triangular flow cross section the hydraulic radius can be shown to be given by

$$R = \frac{1}{2} \sin \alpha h$$

where 2α is the angle of intersection of the channel walls. Thus,

in this case $C = \frac{1}{n} \left(\frac{\sin \alpha}{2} \right)^{\frac{2}{3}}$ and no approximation is made in

assuming a relationship like equation (A5) for the hydraulic radius and C is no longer a function of flow height. However, notice that for triangular cross-sectional forms the continuity equation (equation 2) changes to

$$h_t + uh_x + \frac{1}{2} hu_x = 0 .$$

APPENDIX II

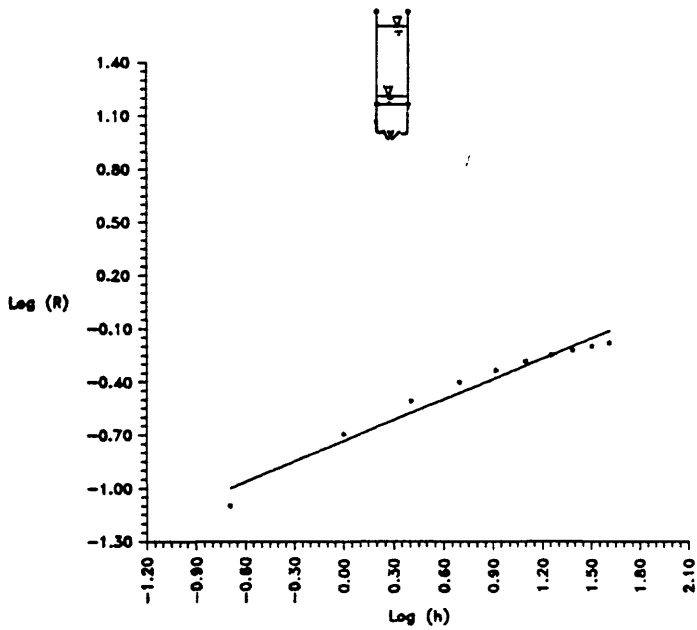
In order to show the dependence of k_1 and a on flow cross-

sectional shape, we have calculated the parameters k_1 and a for eight different cross sectional forms (Figs. 10 and 11) using equation (A5) for hydraulic radius in terms of flow height, that is $R = ah^{k_1}$. We have determined values of the hydraulic radius, the ratio of flow cross-sectional area to wetted perimeter, for these eight sections, for values of fluid height ranging from 0.5 to 5 m, a range of fluid height that can reasonably account for many real cases. For each section one value of R was calculated every 0.5 m. These were then plotted against h in bilogarithmic planes and linear regressions were performed for k_1 and a for every cross sectional form. Values for the squared correlation coefficient are also shown in Figs. 10 and 11.

The first four sections are rectangular sections with widths w of 2, 8, 16 and 32 m, respectively. Linear regressions for these four sections are shown in Fig. 10. It is easily seen that the width of the cross section affects both k_1 and a ; the narrower the rectangular cross section the smaller are the values for k_1 and a . We can show that a ranges between 0, for rectangular flow cross sections of zero width, and 1, for rectangular cross sections of infinite width. Notice from Fig. 10 that the correlation coefficient is higher for larger widths: the larger the rectangular cross section the better equation (A5) expresses R .

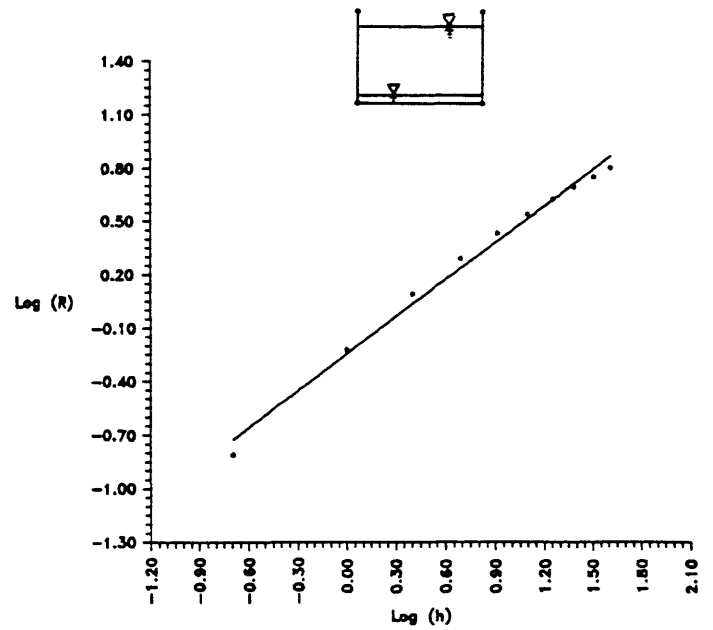
We have also determined the values for k_1 and a for four different trapezoidal sections (Fig. 11) using equation (A5). Observe that equation (A5) gives better results for trapezoidal sections than for rectangular sections: the correlation coefficient is high also for sections with small basal width b (Figs. 11a and 11b). However, remember that in order to approximate the cross-sectional form with a trapezium the continuity equation (equation 2) needs to be changed.

The parameter k_1 depends on the cross section basal width, b , in the trapezoidal case. In fact for the same b value a larger z ($z = \cot\alpha$, where α is the slope of the side) gives a larger k_1 value (Figs. 11 a and b). Notice that, on the contrary,



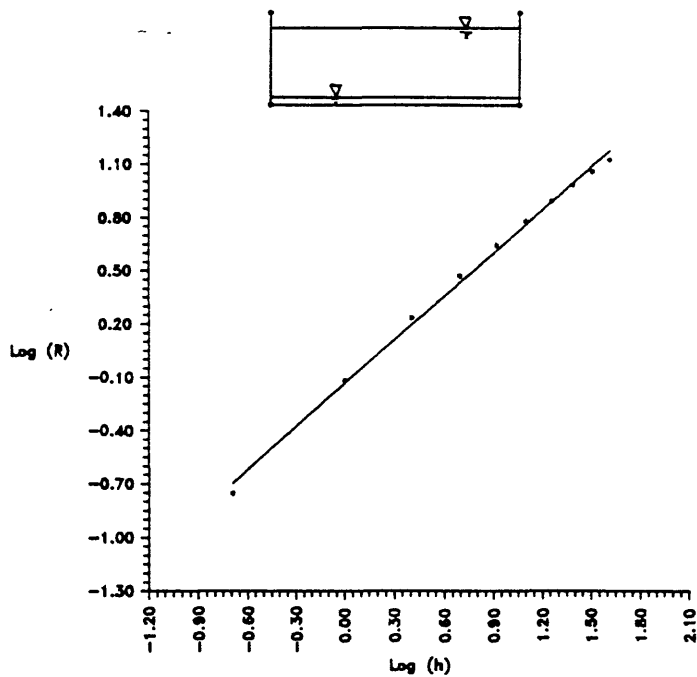
a) rect. section, $b = 2$ $r^2 = 0.960$

$a = 0.481$ $k_1 = 0.383$



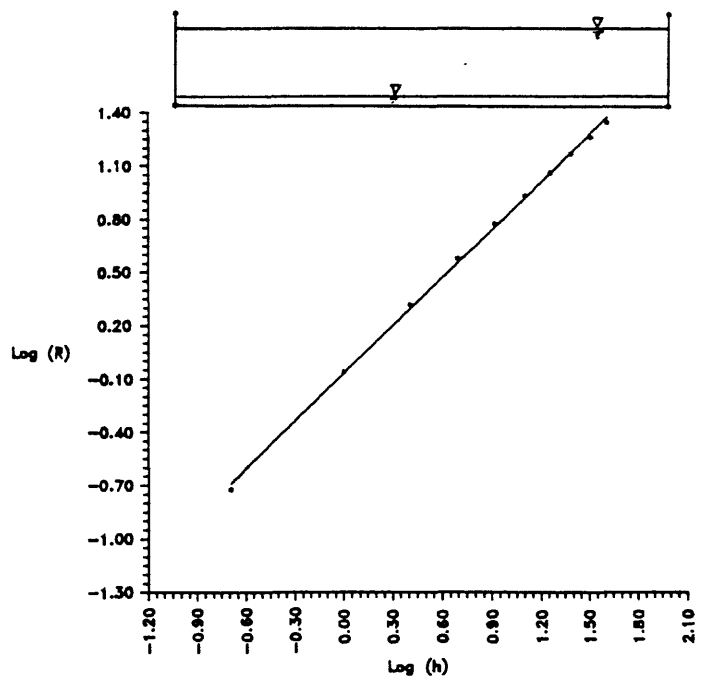
b) rect. section, $b = 8$ $r^2 = 0.991$

$a = 0.781$ $k_1 = 0.691$



c) rect. section, $b = 16$ $r^2 = 0.996$

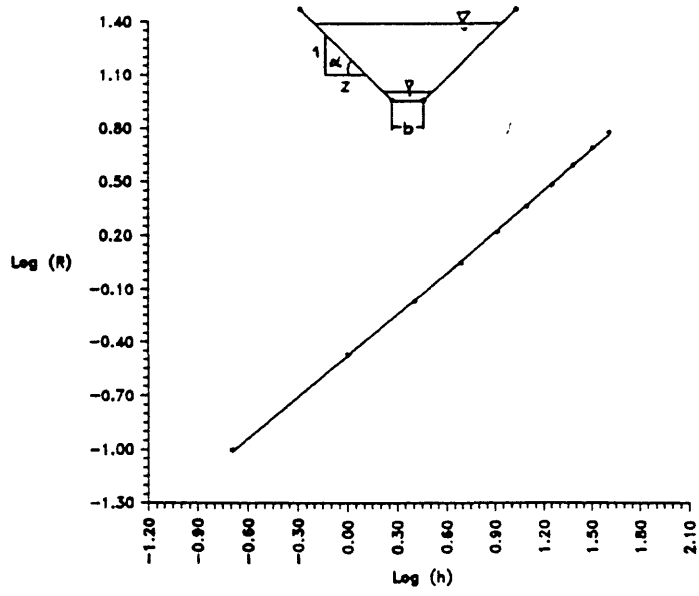
$a = 0.876$ $k_1 = 0.812$



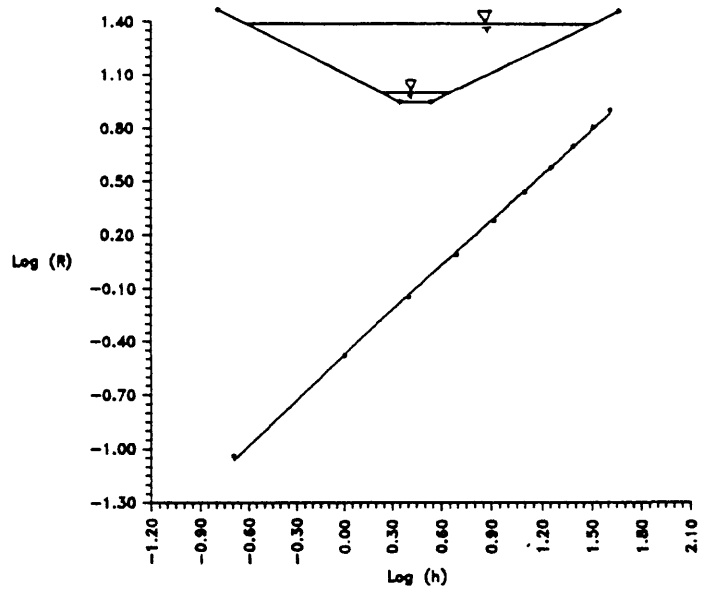
d) rect. section, $b = 32$ $r^2 = 0.999$

$a = 0.934$ $k_1 = 0.894$

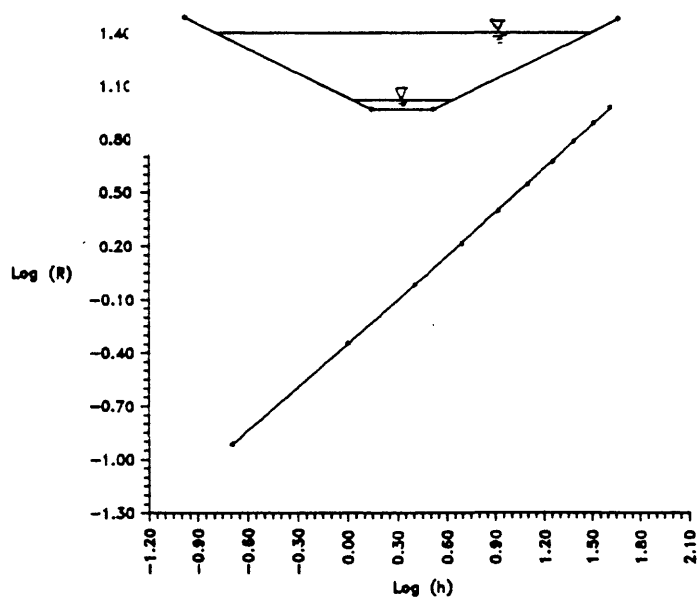
Figure 10. - Bilogarithmic linear regressions of hydraulic radius against flow height for four different rectangular sections and respective a and k_1 values.



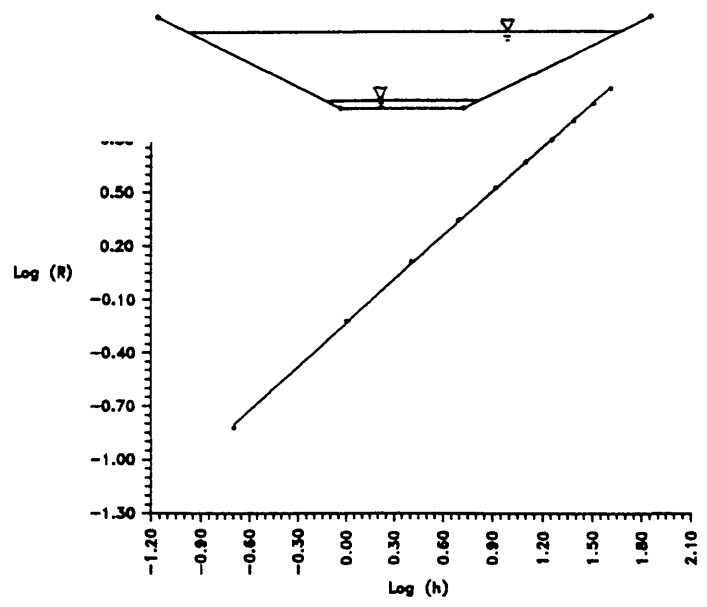
a) trapez. section, $b = 2, z = 1$ $r^2 = 0.9998$
 $a = 0.619$ $k_1 = 0.770$



b) trapez. section, $b = 2, z = 2$ $r^2 = 0.9995$
 $a = 0.621$ $k_1 = 0.844$



c) trapez. section, $b = 4, z = 2$ $r^2 = 0.99996$
 $a = 0.705$ $k_1 = 0.818$



d) trapez. section, $b = 8, z = 2$ $r^2 = 0.9997$
 $a = 0.793$ $k_1 = 0.824$

Figure 11. - Bilogarithmic linear regressions of hydraulic radius against flow height for four different trapezoidal sections and respective a and k_1 values.

the coefficient a does not change significantly with side slope. Observe also that the k_1 values in this case are much larger than for a rectangular section in which the width w is the same value as b .

The k_1 value expresses the closeness of the section to a triangular form. For triangular sections $k_1 = 1$. For the same side slope the k_1 value for the section of Fig. 11b is larger than the k_1 value for the sections of Fig. 11c and 11d, despite the fact that they have larger b values. This can be explained by observing that the cross section whose linear regression is shown in Fig. 11b is much closer to a triangular form than the cross sections of Figs. 11c and 11d.

The coefficient α is less affected by the closeness of the section to a triangular form. It increases with b and is not much influenced by the side slope.

REFERENCES

- Abbott, M. B., 1966, An introduction to the method of characteristics: New York, American Elsevier, 243 p.
- Bagnold, R. A., 1954, Experiments on a gravity-free dispersion of large solid spheres in a Newtonian fluid near shear: Proceedings, Royal Society of London, ser. A, v. 225, p. 49-63.
- Bingham, E. C., 1922, Fluidity and plasticity: New York, McGraw-Hill Book Co., 440 p.
- Chen, C. L., 1987, Comprehensive review of debris flow modeling concepts in Japan, in Costa, J. E. and Wieczorek, G. F. eds., Debris flow/avalanches: process, recognition and mitigation: Geological Society of America, Reviews in Engineering Geology, v. 7, p. 13-29.
- Chen, C. L., 1988, Generalized viscoplastic modeling of debris flow: American Society of Civil Engineers, Journal of Hydraulic Engineering, v. 114, no. 3, p. 237-258.

- Chow, V. T., 1959, Open-channel hydraulics: New York, McGraw-Hill Book Co., 680 p.
- Costa, J. E. and Williams, G. P., 1984, Debris-flow dynamics: U.S. Geological Survey Open-File Report 84-606, Video Tape, 23 min.
- Gallino, G. L., and Pierson, T. C., 1984, The 1980 Polallie creek debris flow and subsequent dam-break flood, east Fork Hood river basin, Oregon: U.S. Geological Survey Open-File Report 84-578, 39 p.
- Hunt, B., 1982, Asymptotic solution for dam-break problem: Journal of the Hydraulics Division, Proceedings of the American Society of Civil Engineers, v. 108, no. HY1, p. 115-126.
- Johnson, A. M., 1970, Physical processes in geology: San Francisco, W. H. Freeman, 577 p.
- Laenen, A., and Hansen, R. P., 1988, Simulation of three lahars in the Mount St. Helens area, Washington, using a one-dimensional, unsteady-state streamflow model: U.S. Geological Survey Water-Resources Investigation Report 88-4004, 20 p.
- Lighthill, M. J., and Whitham, G. B., 1955, On kinematic waves I. Flood movement in long rivers: Proceedings of the Royal Society of London, v. A 229, p. 281-316.
- Pierson, T. C., 1986, Flow behavior of channelized debris flows, Mount St. Helens, Washington: in Abrahms, A. D., ed., Hillslope Processes: Boston, Allen & Unwin, p. 269-296.
- Pierson, T. C., Janda, R. J., Thouret, J., and Borrero, C. A., 1990, Perturbation and melting of snow and ice by the 13 November 1985 eruption of Nevado del Ruiz, Colombia, and consequent mobilization, flow and deposition of lahars: Journal of Volcanology and Geothermal Research, v. 41, p. 17-66.
- Rodine, J. M. and Johnson, A. M., 1976, The ability of debris, heavily freighted with coarse clastic materials, to flow on gentle slopes: Sedimentology, v. 23, p. 213-234.
- Rouse, H., 1938, Fluid mechanics for hydraulic engineers: New York, McGraw-Hill Book Co., 422 p.
- Takahashi, T., 1978, Mechanical characteristics of debris flow: Journal of the Hydraulics Division, Proceedings of the American Society of Civil Engineers, v. 104, no. HY8, p. 1153-1169.

- Takahashi, T., 1980, Debris flow on prismatic open channel: Journal of the Hydraulics Division, Proceedings of the American Society of Civil Engineers, v. 106, no. HY3, p. 381-398.
- Varnes, D. J., 1978, Slope movement types and processes, in Schuster, R. L. and Krizek, R. J., eds., Landslides, analysis and control: Washington D. C., National Academy of Sciences, p. 11-33.
- Weir, G. J., 1982, Kinematic wave theory for Ruapehu lahars: New Zealand Journal of Science, v. 25, p. 197-203.
- Weir, G. J., 1983, The asymptotic behavior of simple kinematic waves of finite volume: Proceedings of the Royal Society of London, vol. A 387, p. 459-467.
- Whitham, G. B., 1955, The effects of hydraulic resistance in the dam-break problem: Proceedings of the Royal Society of London, v. A 227, p. 399-407.
- Yano, K., and Daido, A., 1965, Fundamental study on mud-flow: Kyoto, Japan, Kyoto University, Bulletin of the Disaster Prevention Research Institute, v. 14, p. 69-83.